HHS Public Access

Author manuscript

J Biomed Nanotechnol. Author manuscript; available in PMC 2017 June 01.

Published in final edited form as:

J Biomed Nanotechnol. 2016 June ; 12(6): 1297–1302.

First *in vivo* testing of compounds targeting Group 3 medulloblastomas using an implantable microdevice as a new paradigm for drug development

Oliver Jonas[1,*,†], **David Calligaris**[2,†], **Kashi Reddy Methuku**[3], **Michael M. Poe**[3], **Jessica Pierre Francois**[4], **Frank Tranghese**[4], **Armen Changelian**[2], **Werner Sieghart**[5], **Margot Ernst**[5], **Daniel A. Pomeranz Krummel**[6], **James M. Cook**[3], **Scott L. Pomeroy**[4], **Michael Cima**[1], **Nathalie YR Agar**[2,7,8], **Robert Langer**[1], and **Soma Sengupta**[9,*]

[1]David H. Koch Institute for Integrative Cancer Research, Massachusetts Institute of Technology, Cambridge, MA 02139

[2]Department of Neurosurgery, Brigham and Women's Hospital, Harvard Medical School, Boston, MA 02115

[3]Department of Chemistry and Biochemistry, University of Wisconsin-Milwaukee, Milwaukee, WI 53211

[4]Department of Neurobiology, Children's Hospital Boston, Boston, MA 02115

[5]Center for Brain Research, Medical University of Vienna, Spitalgasse 4, A-1090 Vienna, Austria

[6]Department of Biochemistry, Brandeis University, Waltham, MA 02453

[7]Department of Radiology, Brigham and Women's Hospital, Harvard Medical School, Boston, MA 02115

[8]Department of Cancer Biology, Dana-Farber Cancer Institute, Harvard Medical School, Boston, MA 02115

[9]Department of Neurology, Division of Neuro-Oncology, Beth Israel Deaconess Medical Center, Harvard Medical School, Boston, MA 02115

[*]Corresponding authors: Soma Sengupta, Phone: 617-667-1665; Fax: 617-667-1664; ssengup1@bidmc.harvard.edu; and Oliver Jonas, Phone: 781-266-7862; Fax: 617-258-8827; ojonas@mit.edu.

[†]These authors contributed equally to this work.

Disclosure of Potential Conflicts of Interest

None of the authors have any conflicts of interests to declare, except for Nathalie Agar who is a scientific advisor to BayesianDx and to inviCRO.

Author's contributions

Conception and design: S. Sengupta and O. Jonas

Development of methodology: R. Langer, M. Cima, N. Agar, J. Cook, S. Sengupta

Acquisition of data & making compounds: O. Jonas, D. Calligaris, K. Reddy Methuku, M. M. Poe, W. Sieghart, M. Ernst, F. Tranghese.

Analysis and interpretation of data (e.g., mass spec data, microreservoir apoptosis data): O. Jonas, D. Calligaris, S. Sengupta

Writing, review, and/or revision of the manuscript: S. Sengupta, O. Jonas, D. Pomeranz Krummel, D. Calligaris, N. Agar, W. Sieghart.

Administrative, technical, or material support: S. Pomeroy, N.Y.R Agar, F. Tranghese, A. Changelian, D. Pomeranz Krummel, J. Pierre Francois

Abstract

Medulloblastoma is the most common childhood malignant brain tumor. The most lethal medulloblastoma subtype exhibits a high expression of the $GABA_A$ receptor α5 subunit gene and MYC amplification. New benzodiazepines have been synthesized to function as α5-$GABA_A$ receptor ligands, but these had undesirable side effects in the nude mouse xenograft model system (4). To compare their efficacy with that of standard-of-care treatments, we have employed a newly developed microscale implantable device that allows for high-throughput localized intratumor drug delivery and efficacy testing. We have identified a benzodiazepine derivative, KRM-II-08, as a new potent inhibitor in several α5-$GABA_A$ receptor expressing tumor models. Obtaining high-throughput drug efficacy data within a native tumor microenvironment as detailed herein, prior to pharmacological optimization for bioavailability or safety and without systemic exposure or toxicity, may allow for rapid prioritization of drug candidates for further pharmacological optimization.

Keywords

medulloblastoma; microdevice; benzodiazepine derivatives; tissues mass spectrometry

Introduction

Medulloblastoma accounts for 10–20 percent of all primary tumors of the central nervous system among children and young adults less than 19 years of age and is found in the posterior fossa (1, 2). The current and most widely used medulloblastoma treatment regimen is highly toxic (1, 2). Children with non-disseminated medulloblastoma (average-risk disease) receive 8 cycles of lomustine (CCNU), vincristine, and cisplatin chemotherapy for approximately 1 year following conventional dose radiotherapy and concomitant vincristine (1, 2). For high-risk disease, patients typically receive standard chemotherapy, including cisplatin, carboplatin, cyclophosphamide, and vincristine, or conventional craniospinal radiotherapy and chemotherapy (1, 2). Unfortunately, this treatment regimen results in significant cognitive problems in children. Further, some children are particularly refractory to such treatment (1, 2). Thus, there is a significant demand for development of alternative therapies, including ones that could function as radiosensitizers so as to reduce the dose of radiation.

Recent genomic studies identified at least four subtypes of medulloblastoma (3). It emerged from these studies that the most lethal medulloblastoma subtype, subgroup 3, exhibits a high expression of the $GABA_A$ receptor α5 subunit gene (GABRA5) and MYC amplification (1–3). Subgroup 3 medulloblastomas are seen primarily in children, have the poorest outcome, and comprise approximately 25 percent of sporadic medulloblastomas. Following the genomic classification, it was shown that α5-$GABA_A$ receptor expression was indeed elevated in this subtype (3). Further, it was observed that treating MYC-driven medulloblastomas with the benzodiazepine QH-II-066, a positive allosteric modulator preferentially interacting with the benzodiazepine binding site of α5-$GABA_A$ receptors, resulted in decreased cell viability and sensitization to cisplatin and gamma irradiation (4). The observation that a α5-GABAA receptor ligand could be an effective radiosensitizer for

subgroup 3 provided impetus for synthesis of new benzodiazepine derivatives that enhance GABA-induced stimulation at α5-$GABA_A$ receptors (5–8). However, the *in vivo* efficacy testing of these benzodiazepine derivatives have been hampered by respiratory depression in the nude mouse intracranial xenograft model system (4).

To overcome the challenge of toxicity of our newly synthesized potential α5-$GABA_A$ receptor ligands and to conduct a rapid drug delivery screen for their efficacy *in vivo*, we have employed a newly developed microscale implantable device that enables high-throughput localized intratumor drug delivery (9). This device is 800 μm in diameter and 4 mm long, is non-toxic, and permits the simultaneous administration of up to 16 compounds intratumorly (9). We have conducted by means of this microdevice, efficacy studies using nude mouse flank xenografts of α5-$GABA_A$ receptor expressing tumors of newly synthesized compounds, and discovered that a new benzodiazepine derivative, KRM-II-08, demonstrated higher *in vivo* activity than the standard-of-care chemotherapy (cisplatin). The microdevice offers a rapid and cost effective way of testing potential chemotherapeutic and targeted compounds *in vivo* without systemic effects and might also find application in the treatment of tumors in patients.

Results

In vivo identification of potent benzodiazepines

We compared the intratumor microdose efficacy of several benzodiazepines (Fig. 1) enhancing the action of GABA at α5-$GABA_A$ receptors (Footnote 1) with other clinically relevant standard-of-care treatments, including cisplatin, mebendazole and the bromodomain inhibitor JQ1, in several tumor models. Nude mice flank xenografts were created using medulloblastoma tumor cell lines (4). Using the described microdevice technology (9), we observed that α5-$GABA_A$ receptor expressing D425 and D283 tumor cell flank xenografts were found to be significantly more sensitive ($p < 0.01$) to benzodiazepine derivatives than the non-α5-$GABA_A$ receptor expressing medulloblastoma DAOY flank xenografts, as evidenced by local apoptosis induction that was 200–400% higher in these models (Fig. 2) (data shown for D425 only, since D283 was similar). Among the benzodiazepine derivatives, D425 tumors are most sensitive to KRM-II-08, a member of a series of new positive allosteric modulators of α5-$GABA_A$ receptors. In addition to high sensitivity to KRM-II-08, the α5-$GABA_A$ receptor expressing tumors are also sensitive to SH-I-75 and QH-II-066, which are members of the same family of compounds. Note that KRM-II-08 and QH-II-066 are chemically almost identical - KRM-II-08 has a 2′-F, whereas QH-II-066 has a 2′-H (Fig. 1). Exposure to KRM-II-08 leads to apoptosis in 38% of exposed cells (apoptotic index, AI) within 24 hours in this model, compared with 21% for SH-I-75 and 13% for QH-II-066 (Fig. 2). KRM-II-08 is also significantly more potent than all other standard-of-care treatments tested in this tumor (Fig. 2). Another α5-$GABA_A$ receptor expressing tumor model, D283, also shows significantly higher local apoptosis induction in response to benzodiazepine derivatives KRM-II-08 (AI = 32%) and QH-II-066 (AI=30%) treatment, compared to other standard-of-care treatments tested. Interestingly, cisplatin (4), JQ1 (10), and mebendazole (11) exhibited a greater effect on the non-α5-$GABA_A$ receptor expressing tumor cell line DAOY (Fig. 2).

Confirmation of locally released drug release distribution? by MALDI mass spectrometry imaging

MALDI mass spectrometry imaging analyses (12, 13) were performed on cross-sectioned mouse frozen flank tissue to demonstrate local drug distribution of compounds released from the microdevice. Figure 3 shows 2-dimensional MALDI mass spectrometry images displaying the distribution of KRM-II-08 (Fig. 3A), QH-II-066 (Fig. 3B), and JQ1 (Fig. 3C) with relative intensities. The high mass accuracy measurement achieved by the FTICR analyzer (better than 1 ppm) enabled confirmation of the release of each compound from the microdevice (Footnote 2). For JQ1, only ions from the fragmentation of the parent molecule were detected during the MALDI MSI analysis. The high laser intensity (i.e. 35%) may be responsible for an in-source fragmentation of the drug.

Based on correlation with a hematoxylin and eosin (H/E) stained serial section, all the compounds were released into the tumor tissue at maximum diffusion distances of 560 μm for JQ1 and greater than 1150 μm for KRM-II-08 and QH-II-066 (Fig. 3; Footnote 3). This area of exposure is approximately congruent with the regions of apoptosis induction that are observed in figure 2, implying that the presence of the drug leads to apoptosis.

Discussion

Rapid identification of drug leads through evaluation of pharmacophore or scaffold constructs *in vivo* may yield rapid prioritization of drug candidates. In this study, we use medulloblastoma tumors to examine a number of previously difficult-to-test new medulloblastoma drugs to study their *in vivo* effects in inducing tumor apoptosis. Compared to *in vitro* testing using cell culture(s), this approach allows drug assessment within the native tumor tissue, thus taking into account microenvironmental factors that contribute to drug response (14).

Compared to traditional systemic dosing studies, this approach allows us to assay test compounds *in vivo* before pharmacological optimization. Importantly, it reduces the number of animals that are needed for such *in vivo* studies by at least one order of magnitude, since multiple drugs can be used in one reservoir, as shown by Jonas *et al*'s recent work (9). In the future, one could envision that this approach may be used in patients for the purpose of more efficient and less toxic drug development if certain safety criteria are met.

To our knowledge, this is the first time where benzodiazepines that enhance the action of GABA at α5-$GABA_A$ receptors have been shown to be effective *in vivo* against the MYC subtype of medulloblastomas, and these appear to be more effective in this kind of screening system than cisplatin, JQ1 and mebendazole, note that the 24 hour timepoint was selected based on prior studies (4, 9). Since allosteric modulators at α5-$GABA_A$ receptors have limited toxicity and have been studied in animal models (8), this makes them attractive to use in the clinical trial setting. The compounds investigated in this study, however, not only modulate α5-$GABA_A$ receptors but also other $GABA_A$ receptor subtypes that also might be expressed in medulloblastoma, but they all exhibit a relatively low activity at the α1-$GABA_A$ receptor subtype (Ernst et al., unpublished results). This is in contrast to diazepam that is only weakly active in inducing apoptosis in medulloblastoma (4). Additional

experiments have thus to be performed to finally identify the receptor subtype(s) eliciting the beneficial effect against medulloblastoma growth and to clarify the exact mechanism of downstream events mediated by these compounds (4).

It is important to note that GABA pathway involvement does occur in several other tumor types, including neuroblastoma (15, 16), pancreatic cancer (17) and lung cancer (18). A rapid screening method testing compounds that can down-regulate GABA signaling could potentially be harnessed for therapies, and this may have implications in a number of cancers.

Materials and Methods

Medulloblastoma cell lines and have been described in Sengupta *et al.* (4). In brief, D425, D283 and DAOY cell lines were passaged in DMEM/F-12 (Dulbecco's Modified Eagle Medium/Nutrient Mixture) with 10% Fetal Bovine Serum, 1% Pen-Strep (10,000 units/mL penicillin & 10,000 ug/mL streptomycin), and 1% of 200 mM L-glutamine. All chemicals were purchased from Life Technologies. Cells were maintained in conditions of 37°C and 5% CO_2 and passaged 1–3 times per week on reaching ~70% confluence. Tumor cells (~3×10^6) in PBS were injected subcutaneously into the flanks above the hind limbs of 6–8 week-old female athymic nude mice (Crl:NU(NCr)-Foxn1^{nu}), purchased from Charles River Laboratories. Tumors grew for approximately 4–5 weeks, to a size of 6–10 mm, before device implantation. All protocols for mouse experiments were approved by the Committee on Animal Care of the Massachusetts Institute of Technology (protocol 0412-038-15).

Microdose drug delivery devices were manufactured as described in Jonas *et al.* (9). In short, cylindrical, micro-scale devices with 0.82 (diameter) × 4 mm (length) were manufactured from medical-grade Delrin acetyl resin blocks (DuPont) by micromachining (CNC Micromachining Center, Cameron). Circular reservoirs (8–12 per device) were shaped on the outer surface of devices in dimensions of 230 μm (diameter) × 250 μm (depth). Drug-polymer mixtures were packed into device reservoirs using a tapered, metal needle (Electron Microscopy Sciences) until the reservoirs were completely filled.

Devices were implanted directly into the mouse tumor using a 19-gauge spinal biopsy needle (Angiotech) and a retractable needle obturator to push the device into the tissue. Devices containing the drug remained *in situ* for 24 hours. Of the drugs, benzodiazapines QH-II-066, KRM-II-08, and SH-I-75 were synthesized at the Department of Chemistry and Biochemistry, University of Wisconsin-Milwaukee. The details of their synthesis have been reported (5, 6). JQ1 was a gift of the Bradner Laboratory, Dana-Farber Cancer Institute (19). Mebendazole and Cisplatin (cis-Diammineplatinum(II) dichloride), Diazepam were purchased from Sigma Aldrich. Each drug reservoir in the microdevice contained approximately 1 μg of the compound.

The flank tumor was excised and the tissue containing the device was fixed for 24 hours in 10% formalin and perfused with paraffin. This specimen was sectioned using a standard microtome and tissue sections were collected from each reservoir. Sections were antibody-stained by standard immunohistochemistry using Cleaved-caspase-3 antibody (Cell

Signaling) and scored using an ImageJ image (v1.48) analysis algorithm in a blinded manner.

For MALDI mass spectrometry imaging, purified matrix 2,5-dihydroxybenzoic acid (DHB) was purchased from Sigma-Aldrich. Flash frozen tissue samples for mass spectrometry were placed at −20°C for 1 hour before sectioning. Tissue sections of 12 μm thickness were prepared using a Microm HM550 cryostat (Thermo Scientific™) with the microtome chamber chilled at −20°C and the specimen holder at −21°C, and thaw mounted onto ITO-coated microscope slides (Bruker Daltonics). Samples were dried for 15 minutes in a desiccator, and subjected to matrix deposition as follows. DHB (160 mg/mL solution in methanol/0.2% TFA 70:30 vol/vol) was deposited using a TM-sprayer (HTX imaging) with a flow rate of 90 μL/min; spray nozzle velocity, 1,200 mm/min; spray nozzle temperature, 75°C; nitrogen gas pressure, 10 psi; track spacing, 2 mm; number of passes, 4.

Mass spectra were acquired using a SolariX XR Fourier transform ion cyclotron resonance mass spectrometer (FTICR MS) (9.4 T) (Bruker Daltonics). The mass spectrometer was externally calibrated using arginine clusters in electrospray ionization positive ion mode. MALDI MSI experiments were acquired with a pixel step size for the surface raster set to 30 μm in the FlexImaging 4.0 software. Spectra were acquired in positive ion mode from 1000 laser shots accumulated at each spot for a mass range m/z 100–2500. The laser intensity was set to 35% with a frequency of 1000 Hz. The MALDI images were displayed using the software FlexImaging 4.0, following the signal of KRM-II-08 (m/z 293.1084 ± 0.001), QH-II-066 (m/z 275.1178 ± 0.001) and a fragment of JQ1 (m/z 401.0833 ± 0.001).

Acknowledgments

Grant Support

This study was supported by the following sources of funding:

- Soma Sengupta’s research was supported by K12CA090354 and K08NS083626 awards.
- Agar laboratory work was funded in part by US National Institute of Health (NIH) Director’s New Innovator Award (1DP2OD007383-01), Dana-Farber PLGA Foundation, and Daniel E. Ponton fund for the Neurosciences to NYRA.
- Scott Pomeroy’s laboratory is supported by R01CA109467.
- Pomeranz Krummel’s laboratory is supported by NSF Award No. 1157892.
- Jim Cook’s research was supported by NIH (NS076517,MH096463) grants, as well as the Bradley-Herschfield Foundation(UWMFDN).
- Langer & Cima Labs: This work was funded in part by a Koch Institute Frontier Award and by NCI grant R21CA177391.
- Margot Ernst laboratory: FWF grants W1232 and P 27746.

All the co-authors would like to thank Dr. J. Bradner’s laboratory for supplying JQ1, and Dr. J. Agar for access to his 9.4 T FTICR mass spectrometer at Northeastern University. S. Sengupta acknowledges the support of the mentors of the K12 committee: Dr. R.L. Martuza (Neurosurgery, MGH), Dr. T. T. Batchelor (Neuro-oncology, MGH), and Dr. P.Y. Wen (Neuro-oncology, DFCI). In addition, Soma Sengupta wishes to thank Dr. C.B. Saper (Chair of Neurology, BIDMC), Dr. K.L. Ligon (Neuropathology, DFCI), T. C. Archer for helpful discussions.

References

1. Pomeroy, SL. Clinical presentation, diagnosis, and risk stratification of medulloblastoma. In: Eichler, AF., editor. UpToDate. UpToDate; Waltham, MA: [Accessed on April 18, 2015]
2. Pomeroy, SL. Histopathology and molecular pathogenesis of medulloblastoma. In: Eichler, AF., editor. UpToDate. UpToDate; Waltham, MA: [Accessed on April 18, 2015]
3. Pugh TJ, Weeraratne SD, Archer TC, et al. Medulloblastoma exome sequencing uncovers subtype-specific somatic mutations within a broad landscape of genetic heterogeneity. Nature. 2012; 488:106–110. [PubMed: 22820256]
4. Sengupta S, Weeraratne SD, Sun H, et al. α5-GABAA receptors negatively regulate MYC-amplified medulloblastoma growth. Acta Neuropathol. 2014; 127(4):593–603. DOI: 10.1007/s00401-013-1205-7 [PubMed: 24196163]
5. Cook, JM., Zhou, H., Huang, S., Sarma, PVVS., Zhang, C. Stereospecific Anxiolytic and Anticonvulsant Agents with Reduced Muscle-Relaxant, Sedative-Hypnotic and Ataxic Effects. 2006. Pub No. US2006/0003995A1
6. Cook, J., Huang, S., Edwankar, R., Namjoshi, OA., Wang, Z. Selective Agents for Pain Suppression. 2010. Pub. No. US2010/0317619A1
7. Huang Q, He X, Ma C, et al. Pharmacophore/receptor models for $GABA_A$/BzR subtypes (α1β3γ2, α5β3γ2, and α6β3γ2) via a comprehensive ligand-mapping approach. J Med Chem. 2000; 43:71–95. [PubMed: 10633039]
8. Clayton T, Chen JL, Ernst M, et al. An updated unified pharmacophore model of the benzodiazepine binding site on aminobutyric $acid_a$ receptors: correlation with comparative models. Curr Med Chem. 2007; 14:2755–2775. [PubMed: 18045122]
9. Jonas O, Landry HM, Fuller JE, Santini JT, Baselga J, Tepper RI, Cima MJ, Langer R. An implantable microdevice to perform high-throughput in vivo drug sensitivity testing in tumors. Sci Transl Med. 2015; 7(284):284ra57.doi: 10.1126/scitranslmed.3010564
10. Bandopadhayay P, Bergthold G, Nguyen B, et al. BET bromodomain inhibition of MYC-amplified medulloblastoma. Clin Cancer Res. 2014; 20(4):912–925. DOI: 10.1158/1078-0432.CCR-13-2281 [PubMed: 24297863]
11. Bai RY, Staedtke V, Rudin CM, et al. Effective treatment of diverse medulloblastoma models with mebendazole and its impact on tumor angiogenesis. Neuro Oncol. 2015; 17(4):545–554. DOI: 10.1093/neuonc/nou234 [PubMed: 25253417]
12. Liu X, Ide JL, Norton I, Marchionni MA, Ebling MC, Wang LY, Davis E, Sauvageot CM, Kesari S, Kellersberger KA, Easterling ML, Santagata S, Stuart DD, Alberta J, Agar JN, Stiles CD, Agar NY. Molecular imaging of drug transit through the blood-brain barrier with MALDI mass spectrometry imaging. Sci Rep. 2013; :3. Article number 2859. doi: 10.1038/srep02859
13. Pokorny JL, Calligaris D, Gupta SK, Iyekegbe DO Jr, Mueller D, Bakken KK, Carlson BL, Schroeder MA, Evans DL, Lou Z, Decker PA, Eckel-Passow JE, Pucci V, Ma B, Shumway SD, Elmquist WF, Agar NY, Sarkaria JN. The Efficacy of the Wee1 Inhibitor MK-1775 Combined with Temozolomide Is Limited by Heterogeneous Distribution across the Blood-Brain Barrier in Glioblastoma. Clin Cancer Res. 2015; 21(8):1916–1924. [PubMed: 25609063]
14. Straussman R, Morikawa T, Shee K, et al. Tumour micro-environment elicits innate resistance to RAF inhibitors through HGF secretion. Nature. 2012; 487(7408):500–504. DOI: 10.1038/nature11183 [PubMed: 22763439]
15. Roberts SS, Mori M, Pattee P, et al. GABAergic system gene expression predicts clinical outcome in patients with neuroblastoma. J Clin Oncol. 2004; 22:4127–4134. DOI: 10.1200/JCO.2004.02.032 [PubMed: 15483022]
16. Hiyama E, Hiyama K, Nishiyama M, Reynolds CP, Shay JW, Yokoyama T. Differential gene expression profiles between neuroblastomas with high telomerase activity and low telomerase activity. J Pediatr Surg. 2003; 38:1730–1734. [PubMed: 14666454]
17. Al-Wadei HA, Al-Wadei MH, Ullah MF, Schuller HM. Celecoxib and GABA cooperatively prevent the progression of pancreatic cancer in vitro and in xenograft models of stress-free and stress-exposed mice. PLoS One. 2012; 7:e43376.doi: 10.1371/journal.pone.0043376 [PubMed: 22916251]

18. Schuller HM, Al-Wadei HA, Majidi M. Gamma-aminobutyric acid, a potential tumor suppressor for small airway-derived lung adenocarcinoma. Carcinogenesis. 2008; 29:1979–1985. DOI: 10.1093/carcin/bgn041 [PubMed: 18310090]

19. Filippakopoulos P, Qi J, Picaud S, et al. Selective inhibition of BET bromodomains. Nature. 2010; 468:1067–73. DOI: 10.1038/nature09504 [PubMed: 20871596]

Significance

We have screened *in vivo* for the first time benzodiazepine derivatives against the most aggressive form of medulloblastoma and identified a new potent inhibitor. The process of rapid screening and establishing efficacy of therapies *in vivo* was achieved by using a newly developed microscale device for delivery in conjunction with tissue mass spectrometry to examine drug distribution.

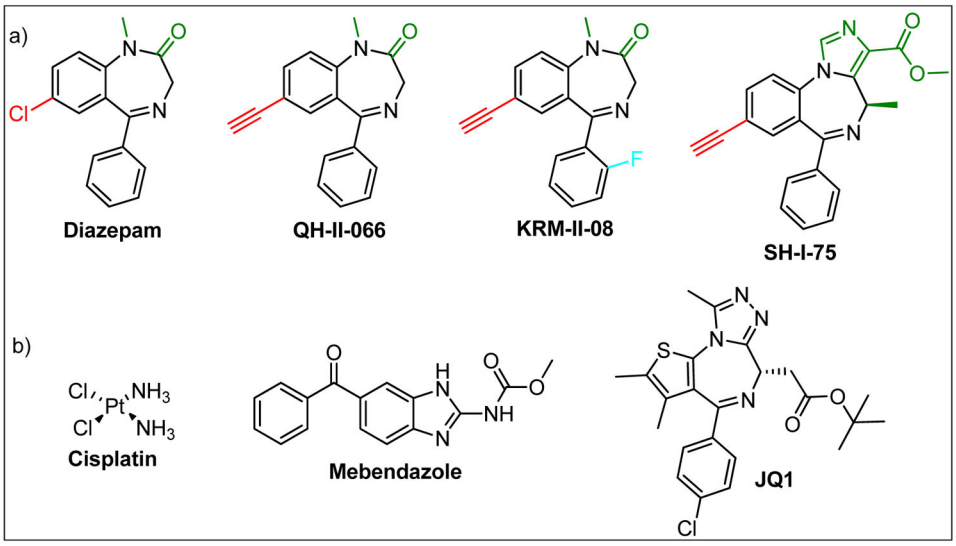

Figure 1. Chemical structures of compounds

A, Structurally related benzodiazepines used in the study. The compounds consist of the core benzodiazepine chemical structure, fusion of benzene and diazepine rings, and structural differences that are highlighted in color. **B,** Chemical structures of the standard-of-care treatment compounds used in the study. JQ1 shares a similar structural format as the benzodiazepine SH-I-75.

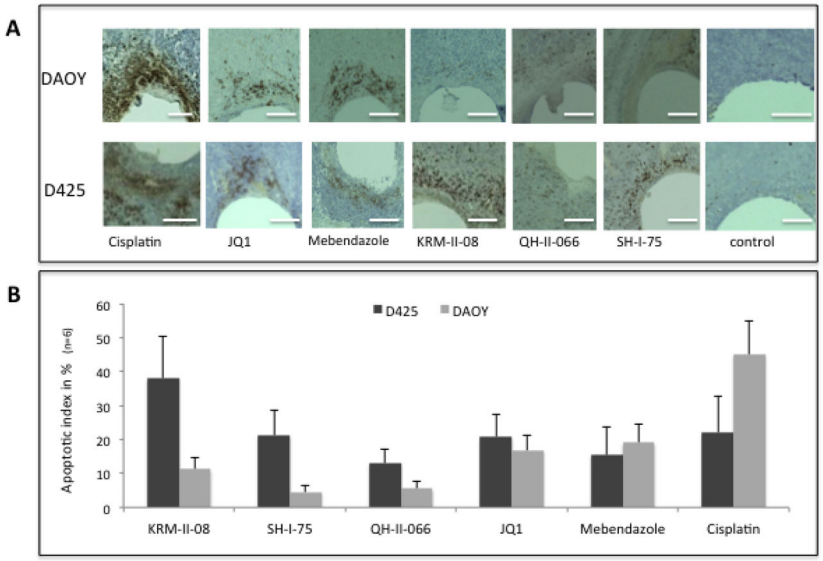

Figure 2. Effect of compounds in microdevice on flank tumors

A, Representative images of D425 and DAOY tumor sections removed 24 hours after exposure to microdose of each drug from the device, showing distinct regions of apoptosis assessed by cleaved-caspase-3 expression (brown) after 24 hours. Scale bars, 250 μm. **B,** Apoptotic index (%apoptotic cells/all cells in drug-affected tissue region) for human D425 and DAOY tumors exposed to KRM-II-08, SH-I-75, QH-II-066, JQ1, mebendazole and cisplatin (all 35% drug in PEG1450). Averages are taken from 6 spatially distinct reservoirs from at least 3 tumors please give ($p < 0.01$).

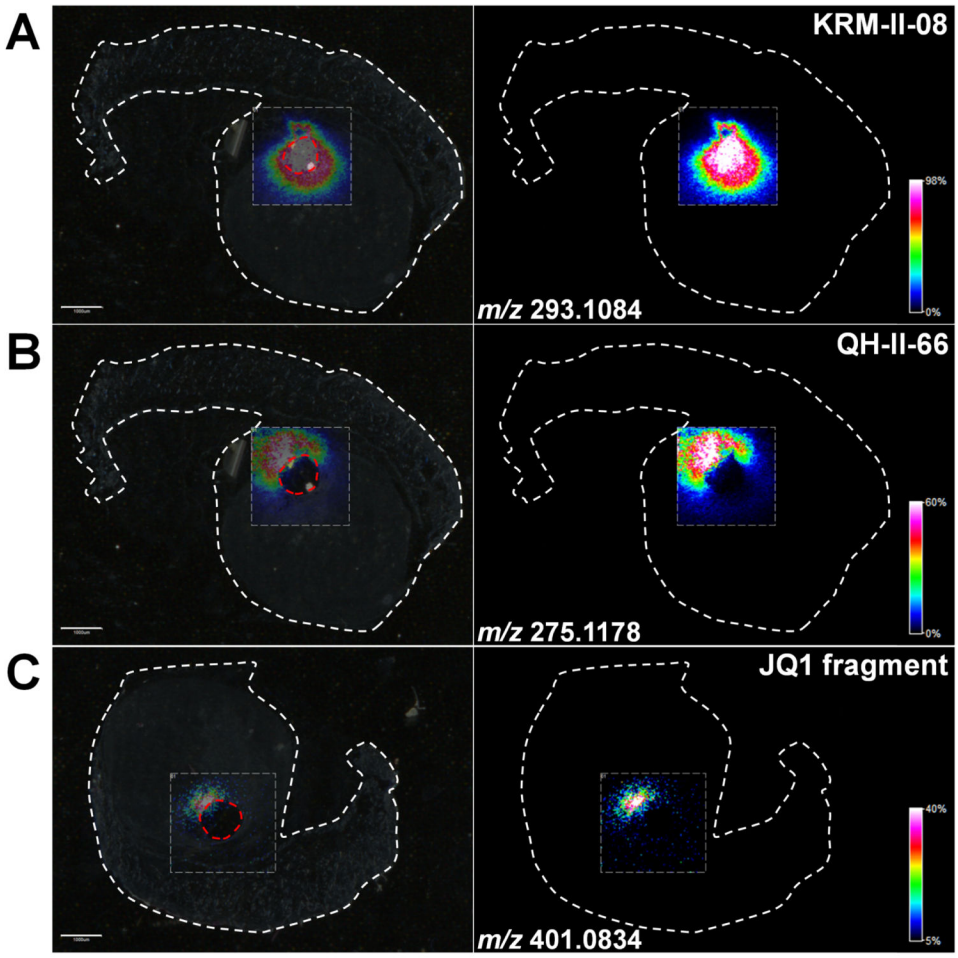

Figure 3. MALDI FTICR mass spectrometry molecular imaging of compound distribution

Matrix-assisted laser desorption/ionization Fourier-transform ion cyclotron resonance (MALDI FTICR) mass spectrometric imaging (MSI) of the distribution of three drugs in sections of a mouse flank tumor with an implanted device: **A**, KRM-II-08 (*m/z* 293.1084); **B**, QH-II-066 (*m/z* 275.1178); and **C**, a fragment of JQ1 (*m/z* 401.0834). Left and right panels show scanned images of the tissue sections overlaid with the MALDI FTICR MSI data and the MALDI FTICR MSI data only, respectively. The position of the device in each section is delineated by red dotted lines. Images were acquired at a spatial resolution of 30 μm. Scale bars, 1000 μm.

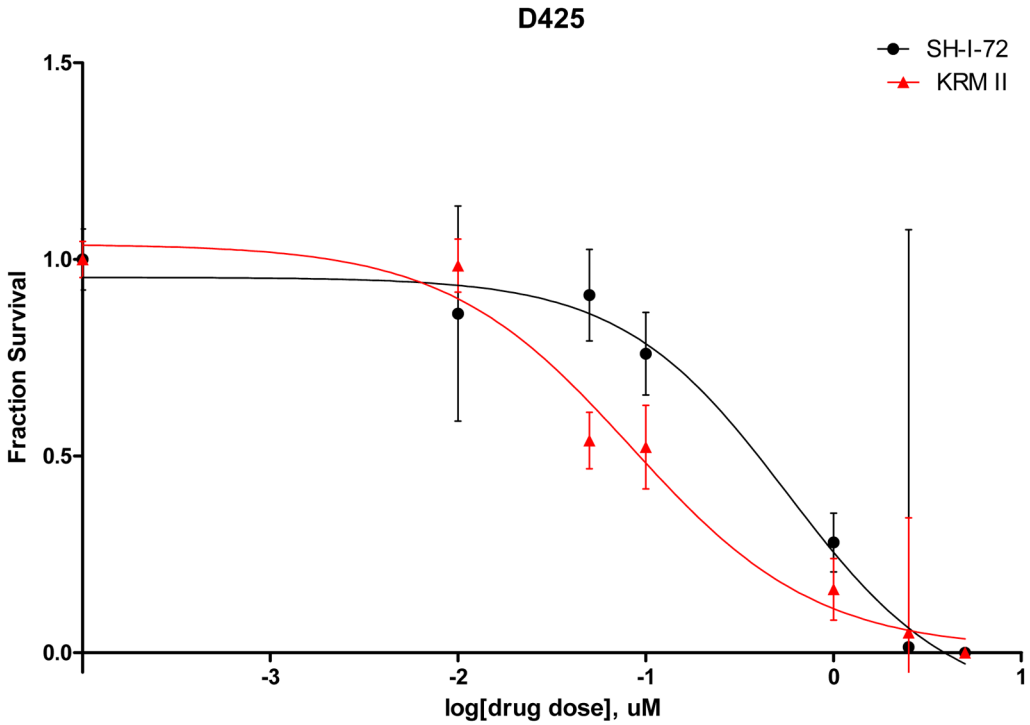

Footnote 1.

Note that the dose response curves for all of the other compounds used in this paper have already been published (4, 10, 11). The dose response curves are shown here for the in vitro assay of medulloblastoma cell line D425 and the compounds used were SH-I-75 and KRM-II-08. Note that D283 produces similar curves, and these drugs do not have an effect on DAOY.

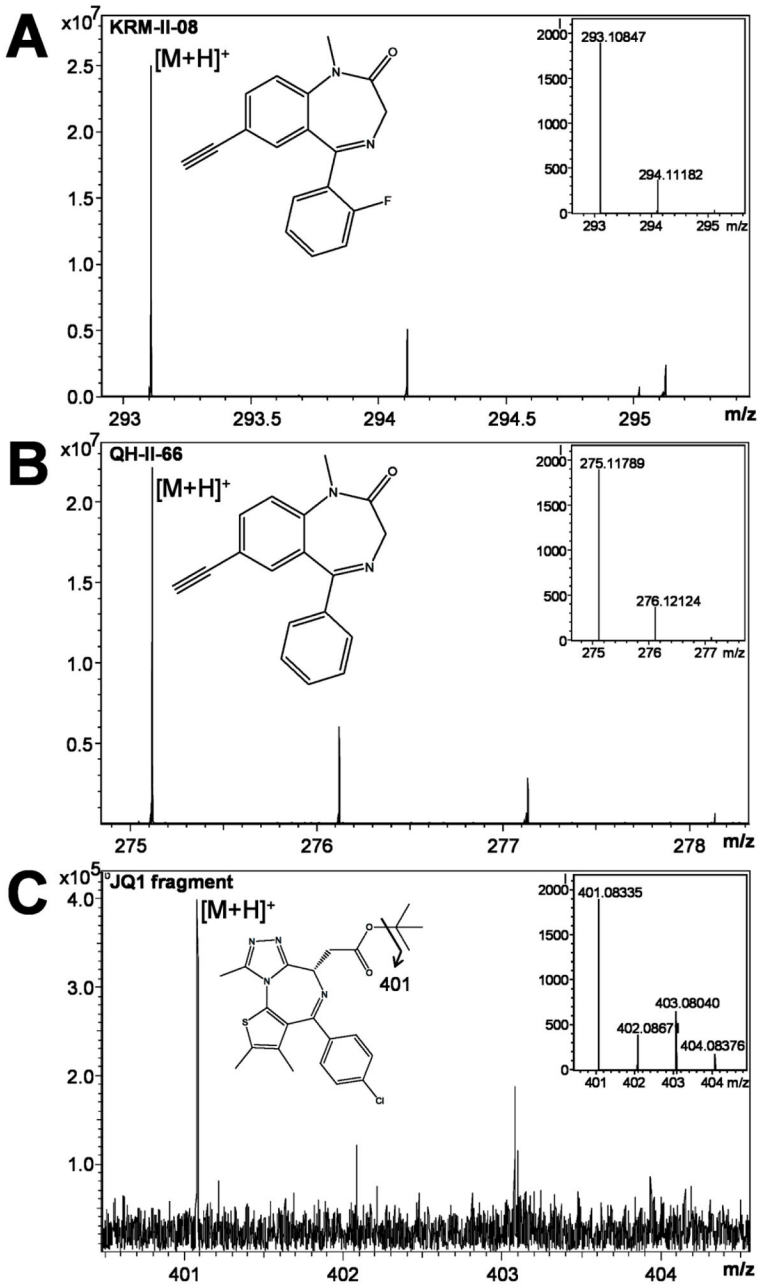

Footnote 2.

MALDI FTICR mass spectra selected from a pixel with maximum intensity in the MS image of figure 3A, 3B, and 3C showing the isotopic distribution of KRM-II-08 (**A**), QH-II-066 (**B**), and a fragment of JQ1 (**C**). Upper right panels display the theoretical isotopic distribution for each compound.

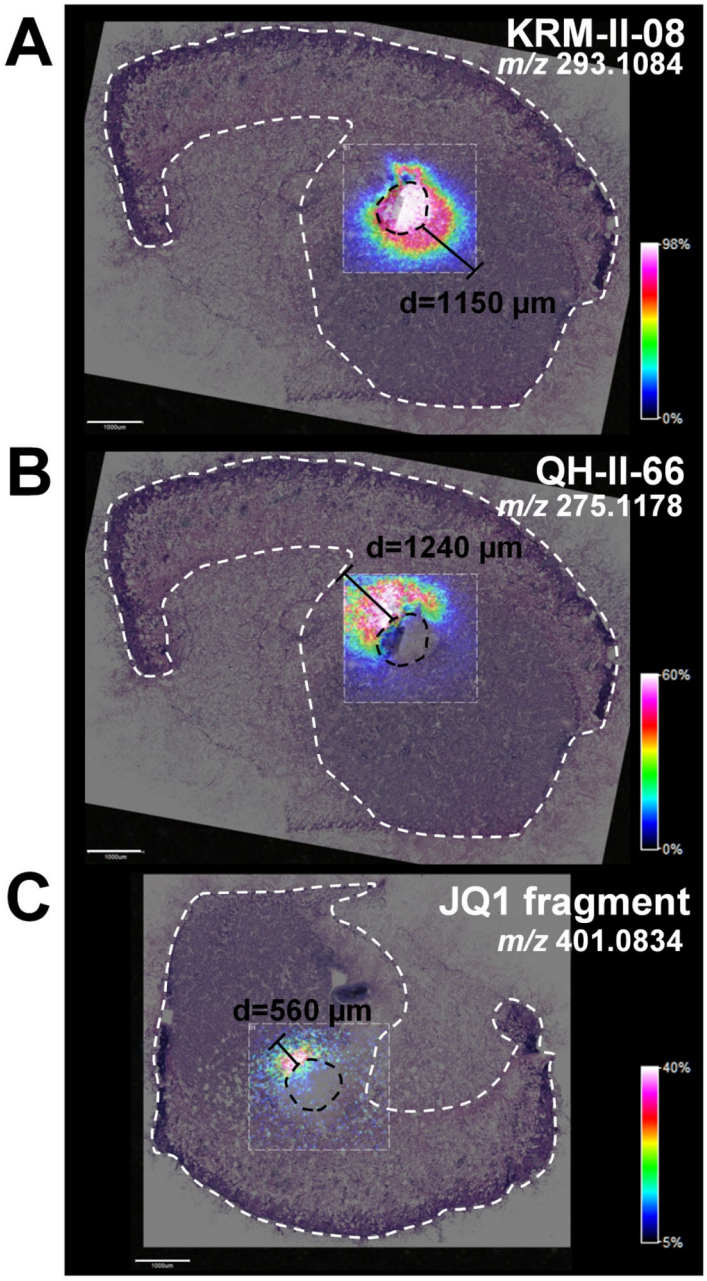

Footnote 3.

MALDI FTICR MSI images representing the distribution of three drugs in sections of a mouse flank tumor with an implanted device: **A**, KRM-II-08 (*m/z* 293.1084); **B**, QH-II-066 (*m/z* 275.1178); and **C**, a fragment of JQ1 (*m/z* 401, 0834). The three panels show scanned images of H/E stained serial sections overlaid with the MSI data. The black lines indicate the diffusion distances (d) within the MALDI MSI measurement region (dotted squares) for each drug. The position of the device in each section is delineated by black dotted lines. Images were acquired at a spatial resolution of 30 µm. Scale bars, 1000 µm. For each serial section, the H/E staining was performed after MALDI matrix removal.